Localization-Oriented Coverage in Wireless Camera Sensor Networks

Liang Liu, Xi Zhang, and Huadong Ma

***Abstract*—In this paper, we investigate the coverage problem from the perspective of target localization for wireless camera sensor networks. We first propose a novel localization-oriented sensing model based on the perspective projection of camera sensors. Based on the sensing model, we propose a new notion of coverage, Localization-oriented coverage (*L*-coverage for short), by using Bayesian estimation theory. Furthermore, we analyze the relationship between the density of camera sensors and the *L*-coverage probability under random deployment where camera sensors are deployed according to a 2-dimensional Poisson process. According to the relationship between the density of camera sensors and the *L*-coverage probability, we derive the density requirements for an expected *L*-coverage probability. We validate and evaluate our proposed models and schemes by simulations.**

***Index Terms*—Wireless camera sensor networks, target localization, coverage, coverage probability, Bayesian estimation.**

I. Introduction

In WIRELESS sensor networks, the coverage is an important problem that has received considerable research attention. Generally speaking, coverage answers the question about quality of service (surveillance) that can be provided by a particular wireless sensor network. In most existing works about coverage for wireless sensor networks, a point is said to be covered if its Euclidean distance to a sensor is within the sensing radius of this sensor. This kind of coverage is only considered as the measure of quality for target/event detecting. In fact, coverage can be subject to a wide range of interpretations. For a given wireless sensor network, there are two main factors to determine the appropriate interpretation of coverage.

1) *Sensing model*. The sensing models of most kinds of sensors (such as temperature sensor, light sensor, and microphone) can be simply considered as a disk, and most existing works about coverage are on the basis of this disk sensing model. However, there still exist some other sensing models which cannot be presented by the disk. The camera sensor is a typical example. More recently, rapid advances in the technologies of camera sensors and embedded processors make it possible to deploy the large-scale wireless camera sensor networks [1], [2], [3] for various applications [4], [5], [6], [7]. The difference of sensing models enables novel approaches to study the coverage problem for wireless camera sensor networks.
2) *Application*. Because the target/event detecting is a basic application of wireless sensor networks [8], coverage is used to measure the quality of detecting in most existing works. However, many applications of wireless sensor networks, including event surveillance and target tracking, rely on the locations of targets. Then, target localization is also important for many applications of wireless sensor networks. It is necessary to investigate the coverage problem from the perspective of target localization, and we call it *Localization-oriented coverage* (*L*-coverage for short). Please note that, throughout the rest of this paper, unless otherwise mentioned, "localization" refers to "target localization".

All above observations motivated us to study the *L*-coverage problem for wireless camera sensor networks. In this paper, we formulate the problem of *L*-coverage in the framework of *parameter estimation*. Camera sensors cooperate to make an estimate of the target's location. In the deployment region of a given camera sensor network, if the location of a point can be reliably estimated, then this point can be claimed to be *L*-covered. The authors of [9], [10] also formulated the coverage problem in the framework of parameter estimation, and they proposed the notion of *information coverage* based on BLUE (Best Linear Unbiased Estimator). Compared to the information coverage, our proposed *L*-coverage in wireless camera sensor networks has two main differences as follows:

- Information coverage is the measure of quality for target/event existence detecting, and the *L*-coverage is the measure of quality for target localization.
- The sensing model of information coverage satisfies that the parameters of a target/event decay with distance linearly. The sensing model of our *L*-coverage is based on the perspective projection model and the camera noise model, which are nonlinear.

Hence, we propose a novel localization-oriented sensing model for camera sensors by taking the perspective projection

Manuscript received July 17, 2008; revised November 8, 2008; accepted January 1, 2009. The associate editor coordinating the review of this paper and approving it for publication was D. Tarchi.

The research reported in this paper was supported in part by the U.S. National Science Foundation CAREER Award under Grant ECS-0348694; the National Natural Science Foundations of China under Grant No.60833009 and No.90612013; and the National High Technology Research and Development Program of China under Grant No. 2006AA01Z304.

L. Liu was with the Networking and Information Systems Laboratory, Department of Electrical and Computer Engineering, Texas A&M University, College Station, Texas 77843, USA. He is now with Beijing University of Posts and Telecomm., Beijing, 100876, China (e-mail: liangliu82@gmail.com).

X. Zhang is with the Networking and Information Systems Laboratory, Department of Electrical and Computer Engineering, Texas A&M University, College Station, TX 77843 USA (e-mail: xizhang@ece.tamu.edu).

H. Ma is with the Beijing Key Lab of Intelligent Telecomm. Software and Multimedia, Beijing University of Posts and Telecomm., Beijing, 100876, China (e-mail: mhd@bupt.edu.cn).

Digital Object Identifier 10.1109/TWC.2010.01.080956

model and the camera noise model into account. Based on this sensing model, we define the notion of *L*-coverage by using *Bayesian estimation theory*. Furthermore, we analyze the relationship between *L*-coverage probability and the density of camera sensors under the random deployment, and derive the density requirement of camera sensors for a given *L*-coverage probability. For the same deployment region of a camera sensor network, we compare the *L*-coverage probability to the classic *K*-coverage probability which is the measure of detecting quality.

Our derived results can be used in both the initial deployment phase and the dynamic reconfiguration phase after camera sensors have been deployed, which are detailed as follows:

- In initial deployment phase: Using our results of *L*-coverage, an appropriate number of camera sensors can be derived, in order to guarantee that most of points in the deployment region are *L*-covered.
- In dynamic reconfiguration phase: For a given deployment of wireless camera sensor networks, our results of *L*-coverage can measure the quality of localization for the deployment region, and then suggest future deployment or reconfiguration schemes for improving the overall quality of target localization.

The rest of this paper is organized as follows. Section II describes the related works. Section III proposes the localization-oriented sensing model for the camera sensor. Section IV defines the localization-oriented coverage (*L*-coverage) on the basis of Bayesian estimation and illustrates the notion of *L*-coverage by using 3 cases. Section V derives the density requirements of camera sensors for a given *L*-coverage probability. Section VI evaluates our proposed models and schemes of *L*-coverage by extensive simulations. The paper concludes with Section VII.

II. Related Works

The coverage problem is studied extensively in the literature [12], and it is also a well-studied problem in wireless sensor networks. The most commonly used sensing model for the coverage problem is the disk model, which assumes that the sensing region for a given sensor is a disk centered around it. A point within the disk sensing region is said to be covered. Paper [13] was the first to apply the computational geometry and Voronoi Diagrams to study coverage for wireless sensor networks. The authors of [14] discussed the necessary and sufficient conditions for grid-deployed sensor networks to cover an unit square region completely. Their results also indicate that, when the number of sensor nodes is large, even if each node is highly unreliable and its transmission distance is small, the sensor network can still maintain connectivity with coverage.

For any positive integer *K*, a point is said to be *K*-covered by a sensor network if it falls in at least *K* sensors' sensing regions. The authors of [15] studied the relationships among the probability of a deployment region being *K*-covered by randomly deployed sensors, the sensing radius, and the number of sensors. The authors of [16] proposed a analytical model to compute the number of sensors needed to achieve an expected *K*-coverage probability, only if the proportion of the sensing radius to the deployment region is known. For guaranteeing *K*-coverage under a dynamic topology of sensor network, the authors of [17], [18] proposed a series of distributed algorithms, which can be used by sensor nodes to decide the states (work or sleep) of themselves during a period to ensure *K*-coverage of every point.

Different from the conventional disk sensing models, we employed a directional sector sensing model in our prior work [20]. The similar works can be found in [23], [25]. The authors of [25] addressed the problem on how to select the optimal number of camera sensors and determine their placement in a given monitored area for multimedia surveillance systems. The authors of [24] focused on the placement of camera sensors with respect to maximizing coverage or achieving coverage at a certain resolution. In [21], [22], we extended the directional sensing model for camera sensor by taking the rotatable direction into account, and then we proposed two effective coverage enhancement algorithms by using convex hull theory and virtual potential field theory, respectively.

In all the above types of coverage, a point is said to be covered if it is within the sensing region of any sensor. In contrast, the authors of [9], [10] proposed a new type of coverage, the information coverage, by using the linear estimation theory, where sensors cooperate to make an estimate or decision for the data to sense at a particular location. The information coverage is based on the linear sensing model. The authors of [10], [11] also studied sensor density requirements for a given information coverage probability with random sensor deployment. They provided an upper bound on the probability that an arbitrary point in a randomly deployed sensor field is not information-covered, and also analyzed the relationship between the sensor density and the average field vacancy.

III. Localization-Oriented Sensing Model

As shown in Fig. 1(a), given a number of randomly deployed camera sensors, our goal is to locate a target as accurately as possible in a ground plane. In order to achieve this goal, we first study how to use camera sensors to locate a target, and then build a localization-oriented sensing model for camera sensors. For simplicity, we make the following assumptions.

A1. All camera sensors follow the same sensing model. We assume that the camera sensors are modeled by the perspective projection, and all camera sensors have the same shape of FOV (field-of-view) region. Additionally, all noises are Gaussian noises with zero mean.

A2. The camera sensors can observe a moving target synchronously [30]. If the target moves with a limited speed, the synchronization can be readily implemented by using the methods proposed in [26].

A3. The message functions and transmissions of messages introduce no information loss [10]. In other words, the quantization/modulation/encoding for measurements and the transmission channels are lossless.

When a camera sensor captures a image frame, it can employ *background subtraction*[1] [28], [29] to identify the

[1]Background subtraction is a commonly used technique for segmenting out objects of interest in a scene for applications such as video surveillance.

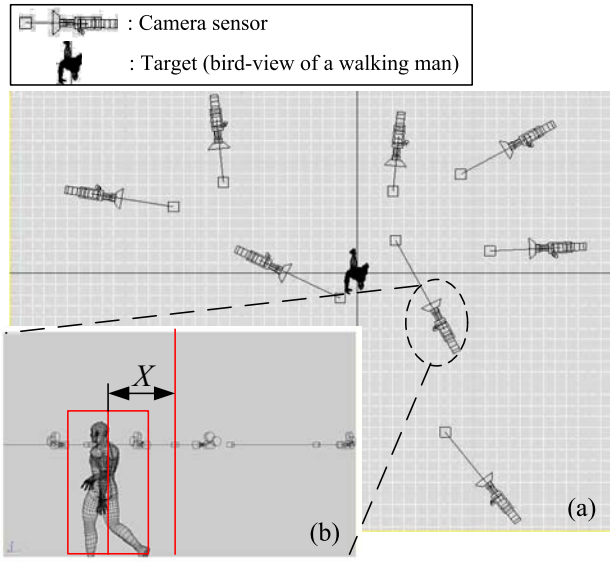

Fig. 1. (a) Schematic of target localization in a camera sensor network. There are several camera sensors deployed in a surveillance region, and a target is in the center of this region. (b) The image captured by the camera sensor which is indicated in the dotted ellipse. The distance, X, from the vertical centerline of the target blob to the centerline of image is the observation measurement by this camera sensor for target localization.

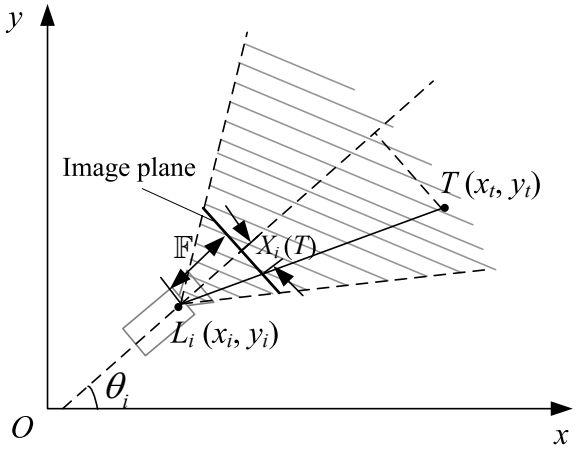

Fig. 2. Perspective projection model.

moving target. As shown in Fig. 1(b), the area of an image frame where there is a significant difference between the observed and estimated images determines the location of a moving object in this image plane. The area containing the change in the frame is further processed to find the horizontal shift, denoted by X, of the target's image from the center of the image plane. In our localization scheme, X is the observation measurement of the camera sensor, and only X is communicated to the central processor (sink node).

Let $T(x_t, y_t)$ be the location of a target. For a given camera sensor c_i, we can get the theoretic horizontal shift, denoted by $\mathbb{X}_i$, of the target image by using the perspective projection model. As shown in Fig. 2, the relationship between $\mathbb{X}_i$ and

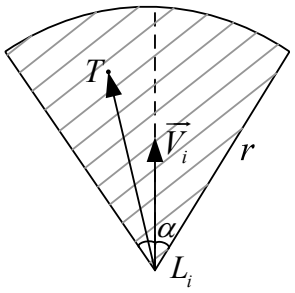

Fig. 3. Sector sensing model.

$T = T(x_t, y_t)$ is

$$\mathbb{X}_i = \mathbb{F} \cdot \tan\left(\theta_i - \arctan\frac{y_t - y_i}{x_t - x_i}\right). \quad (1)$$

The descriptions of parameters used in Eq. (1) are summarized in Table I.

When the distance between the target location T and the camera sensor location L_i becomes far enough, the background subtraction cannot segment out the objects of interest. This implies that the camera sensor c_i cannot detect the target on T. Let r be the maximum detecting distance. Because $r \gg \mathbb{F}$, we employ a sector model to describe the sensing region of a camera sensor. Here, we use D_i to denote the sensing region of c_i. If a point belongs to D_i, then the point can be detected by c_i. As shown in Fig. 3, the sector model can be denoted by a 4-tuple $\left(L_i, r, \overrightarrow{V_i}, \alpha\right)$, where $\overrightarrow{V_i}$ is the unit vector, which evenly splits the sensing sector into two halves, determining sensing direction[2], and α is the offset angle in the field of view on both sides of $\overrightarrow{V_i}$. The point T is said to be covered if and only if 1) $|L_i - T| \leq r$ and 2) the angle between $\overrightarrow{L_iT}$ and $\overrightarrow{V_i}$ is within $[-\alpha, \alpha]$, where $|L_i - T|$ is the Euclidean distance between L_i and T.

From Eq. (1), we can obtain

$$\frac{y_t - y_i}{x_t - x_i} = \tan\left(\theta_i - \arctan\frac{\mathbb{X}_i}{\mathbb{F}}\right). \quad (2)$$

If there is only one measurement, i.e., there is only one camera sensor that can detect the target, then the values of x_t and y_t cannot be uniquely determined because there are two unknowns with just one equation Eq. (2). Thus, we need at least two measurements to uniquely determine the location of the target. Similar to the K-coverage in literatures, the target is K-covered in wireless camera sensor networks if it falls in at least K sector-based sensing regions. Theoretically, from Eq. (2) it appears that the L-coverage problem is equal to the K-coverage problem where $K = 2$. However, this statement is not true, because the the projection model used in Eq. (1) is just an ideal model. The measurement X_i of camera sensor c_i can be corrupted by some additive noises in practice. This implies that only two or even more than two measurements cannot guarantee the target to be located accurately when the noises are large (Thus, K-coverage with $K = 2$ is not L-coverage). These noises mainly come from two aspects: the sensing model of camera sensors and the processing of

[2] θ_i is the directional angle of $\overrightarrow{V_i}$.

TABLE I
PARAMETERS OF PERSPECTIVE PROJECTION.

Parameters	Descriptions
$T(x_t, y_t)$	Location of target in ground plane
$L_i(x_i, y_i)$	Location of camera sensor c_i in ground plane
$X(L_t)$	Horizontal shift of the target's image from the center of the image plane
θ_i	Rotatable angle of camera sensor c_i around x-axis, i.e., the orientation of c_i
$\mathbb{F}$	Focal length of camera sensor

background subtraction. Referring to [27], we assume that the measurement error variance, denoted by σ_i^2, for camera sensor c_i is of the following form:

$$\sigma_i^2 = \zeta d_i^2 + \sigma_p^2 + \sigma_s^2. \tag{3}$$

In Eq. (3), d_i is the distance from the camera sensor c_i to the target. Making camera noise variance dependent on distance can efficiently model the weak perspective projection while allowing the usage of projective model in Eq. (1). Our noise model takes the errors in the calibration of camera sensors into account. Errors in the location of camera sensor c_i are contained in σ_p^2, and errors in the sensor's orientation are measured in ζ. Moreover, the accuracy of background subtraction method and posture/motion of the target also cause errors, and these errors are reflected in σ_s^2.

Therefore, we adopt the Gaussian error model to represent the relationship between the measurement X_i of camera sensor c_i, and the location T of the target. Then, the conditional probability density function of the random measurement variable X_i given T is determined as follows:

$$f(\mathcal{X}_i \mid T) = \frac{1}{\sqrt{2\pi}\sigma_i} \exp\left(-\frac{(\mathcal{X}_i - \mathbb{X}_i)^2}{2\sigma_i^2}\right). \tag{4}$$

IV. BAYESIAN ESTIMATION BASED L-COVERAGE

A. L-Coverage Concept

Consider a deployment field S and a set of N geographically distributed camera sensors. Let $T \in S$ be the location of a target. If T can be detected by k ($0 \le k \le N$) camera sensors simultaneously, then we call these k camera sensors $\{c_1, c_2, \ldots, c_k\}$ a detecting set, denoted by $\mathcal{C}_k$, of the camera sensors for T. This implies that k measurements are available. Assume that the priori probability distribution of T obeys the uniform distribution in S. Then, for an arbitrary point $t(x, y)$ in the two-dimensional space, the probability density function of T is

$$f(t) = \begin{cases} \dfrac{1}{\|S\|}, & t \in S; \\ 0, & t \notin S, \end{cases} \tag{5}$$

where $\|S\|$ denotes the area of S. According to Eq. (4), we have the measurement expression as follows:

$$X_i = \mathbb{X}_i + e_i, \forall i \in \{1, 2, \ldots, k\},$$

where e_i is the additive noise of X_i, and e_i follows the normal distribution of $N(0, \sigma_i)$.

Let $\mathbf{X} \triangleq (\mathcal{X}_1, \mathcal{X}_2, \ldots, \mathcal{X}_k)$ be an arbitrary point in the k-dimensional space of $(X_1, X_2, \cdots, X_k)$. Because the measurements $(X_1, X_2, \cdots, X_k)$ are *i.i.d.*, from Eq. (4) we obtain

$$\begin{aligned} f(\mathbf{X}|t) &= \prod_{i=1}^{k} f(\mathcal{X}_i|t) \\ &= \begin{cases} \displaystyle\prod_{i=1}^{k} \frac{1}{\sqrt{2\pi}\sigma_i} e^{-\frac{(\mathcal{X}_i - \mathbb{X}_i)^2}{2\sigma_i^2}}, & \text{if } k \text{ cameras detect } t; \\ 0, & \text{otherwise.} \end{cases} \end{aligned} \tag{6}$$

According to Eq. (5), Eq. (6), and the Bayesian formula, we get:

$$f(t|\mathbf{X}) = \frac{f(\mathbf{X}|t)f(t)}{\int\int_S f(\mathbf{X}|t)f(t)\mathrm{d}x\mathrm{d}y} = \frac{f(\mathbf{X}|t)}{\int\int_S f(\mathbf{X}|t)\mathrm{d}x\mathrm{d}y}. \tag{7}$$

Let $\widehat{T}_k \triangleq (\widehat{x}, \widehat{y})$ and $\widetilde{T}_k \triangleq |\widehat{T}_k - T|$ denote the estimate and the estimation error for a given measurement $(X_1, X_2, \cdots, X_k)$, respectively, where $|\widehat{T}_k - T|$ is the Euclidean distance between $\widehat{T}_k$ and T, i.e., $\widetilde{T}_k = |\widehat{T}_k - T| = \sqrt{(\widehat{x} - x_t)^2 + (\widehat{y} - y_t)^2}$. The mean square error (MSE) is a common measure of estimator quality. A well-known Bayesian estimator can be applied to estimate $\widehat{T}_k$ and to achieve the minimum MSE. Then, we have the following lemma.

Lemma 1: The Minimum MSE estimator specified by Eq. (7) is determined by

$$\begin{aligned} \widehat{T}_k &= (\widehat{x}, \widehat{y}) \\ &= \left(\frac{\int\int_S x f(\mathbf{X}|t)\mathrm{d}x\mathrm{d}y}{\int\int_S f(\mathbf{X}|t)\mathrm{d}x\mathrm{d}y}, \frac{\int\int_S y f(\mathbf{X}|t)\mathrm{d}x\mathrm{d}y}{\int\int_S f(\mathbf{X}|t)\mathrm{d}x\mathrm{d}y}\right). \end{aligned} \tag{8}$$

Proof: The detailed proof of this lemma is provided in Appendix I. ∎

We use the mean of $\widetilde{T}_k$, denoted by δ_k, to measure how well the point T is located by $\mathcal{C}_k$, which is determined by

$$\delta_k \triangleq \mathrm{E}[\widetilde{T}_k] = \int_{\Re} \widetilde{T}_k f(\mathbf{X}|t)\mathrm{d}\mathbf{X}, \tag{9}$$

where $\widetilde{T}_k = |\widehat{T}_k - T|$, $\Re$ is the k-dimensional real-number space of $(X_1, X_2, \cdots, X_k)$, and the conditional pdf $f(\mathbf{X}|t)$ is a function of r, α, and the other parameters. The smaller δ_k is, the more accurate the estimate is. We assume that the accuracy of localization satisfies the requirement if δ_k is not larger than a predefined threshold ε, i.e., $\delta_k \le \varepsilon$. Then, we can define the notion of *L*-coverage as follows:

Definition 1: Localization-oriented coverage, also called L-coverage. A point is said to be *L*-covered if there exist k camera sensors to estimate the location of this point, and the mean estimate error δ_k satisfies $\delta_k \le \varepsilon$, where $0 < k \le N$.

Remarks on Definition 1: The value of ε is determined by the localization application. On the other hand, ε is generally

TABLE II
THE VALUES OF RELATED PARAMETERS. WE USE SONY DSC-F717 AS THE CAMERA SENSOR IN THE EXPERIMENTS.

Parameters	Values
$\mathbb{F}$	9.45mm
CCD	8.8mm×6.6mm
Angle of view	100°
r	4000mm
$T(x_t, y_t)$	(1950mm,650mm)
ζ	5×10^{-8}
σ_p	0.1
σ_s	0.1
ε	1000mm

relevant to the sensing radius r. For example, if $r = 100$ and $\varepsilon = 100$, the localization accuracy is relatively low; if $r = 1000$ and $\varepsilon = 100$, the localization accuracy is relatively high. Then, we also define the ratio variable $a \triangleq \varepsilon/r$ to measure the requirement of localization accuracy. In Section IV-B, we will use an example to further illustrate the proposed *L*-coverage model.

B. L-Coverage Illustrations

As shown in Fig. 4, we deploy 10 camera sensors in a rectangular region. The values of related parameters are listed in Table II. In Fig. 4, $c_i(x_i, y_i, \theta_i)$ denotes the location and orientation of camera sensor c_i. There are two cases that a camera sensor cannot detect the target on T: 1) T is out of this camera sensor's AOV (angle of view), see camera sensor c_4 in Fig. 4; or 2) the distance between T and the camera sensor exceeds r, see c_5 in Fig. 4.

Let u_i denote the horizontal pixel coordinates of the target for camera sensor c_i. We use three camera sensors c_1, c_2, and c_3, to make measurements, and thus the corresponding horizontal pixel coordinates of the target are $u_1 = 140$, $u_2 = 1055$, and $u_3 = 990$, respectively, as shown in Fig. 4. We first need to transform these pixel coordinates u_i of the horizontal shifts into the real-world coordinates X_i. Because the resolution of these camera sensors is 1280×960 and the size of the Charge Coupled Device (CCD) is 8.8mm×6.6mm, the transformation formula is as follows:

$$X_i = \left(u_i - \frac{1280}{2}\right) \times \frac{8.8}{1280}. \tag{10}$$

Next, we determine whether T is *L*-covered or not by using 3 different detecting sets of camera sensors, respectively.

***Case* I:** $\mathcal{C}_1 = \{c_1\}$

We first use one measurement to estimate the location of target. According to Eq. (1) and Eq. (3), $X_1(T) = -3.15$ and $\sigma_1 = 0.48$, respectively.

Substituting $u_1 = 140$ into Eq. (10), we get $X_1 = -3.4375$. According to Eq. (7), we get the probability distribution function $f(t| - 3.4375)$. When $X_1 = -3.4375$, using Eq. (8) the corresponding minimum MSE $\widehat{T}_1 = (4774.89, 1460.8)$. According to $f(X_1|(1950, 650))$ and Eq. (9), we get $\delta_1 = 2953$mm. Because δ_1 exceeds the threshold $\varepsilon = 1000$mm, T cannot be *L*-covered by the camera sensor c_1.

***Case* II:** $\mathcal{C}_2 = \{c_1, c_2\}$

The detecting set $\mathcal{C}_2 = \{c_1, c_2\}$ implies that we locate the target by combing the measurements of c_1 and c_2. From Eq. (1) and Eq. (3), we can get $\sigma_1 = 0.48$, $\sigma_2 = 0.48$, $X_1(T) = -3.15$, and $X_2(T) = 3.15$. Substituting $u_1 = 140$ and $u_2 = 1055$ into Eq. (10), the measurements of c_1 and c_2 are -3.4375 and 2.8531, respectively. The corresponding $\widehat{T}_2 = (3584, 753)$.

According to $f(X_1, X_2|(1950, 650))$ and Eq. (9), we get $\delta_2 = 1607$mm. In this case, δ_2 also exceeds the threshold 1000mm, and thus T cannot be *L*-covered by $\{c_1, c_2\}$.

***Case* III:** $\mathcal{C}_2 = \{c_1, c_3\}$

In this case, we locate the target by combing the measurements of c_1 and c_3. From Eq. (1) and Eq. (3), $\sigma_1 = 0.48$, $\sigma_3 = 0.75$, $X_1(T) = -3.15$, and $X_3(T) = 1.89$. Substituting $u_1 = 140$ and $u_3 = 990$ into Eq. (10), $X_1 = -3.4375$ and $X_3 = 2.4063$. The corresponding $\widehat{T}_2 = (2246.95, 820.089)$.

According to $f(X_1, X_3|(1950, 650))$ and Eq. (9), we get $\delta_2 = 261$mm< 1000mm. This implies that T can be *L*-covered by $\{c_1, c_3\}$.

V. L-COVERAGE PROBABILITY IN RANDOMLY DEPLOYED WIRELESS CAMERA SENSOR NETWORKS

We consider the random deployment where camera sensors are randomly scattered within a vast two-dimensional geographical region, and their locations are uniformly and independently distributed in the region. Under this deployment strategy, the locations of camera sensors can be modeled by a two-dimensional stationary Poisson point process with intensity λ. This indicates that the number, $N(S')$, of camera sensors in any sub-region S' follows a Poisson distribution with a parameter $\lambda\|S'\|$, where $\|S'\|$ is the area of S'. Let k be a positive integer, the probability that $N(S')$ is equal to k is then given by

$$\Pr\{N(S') = k\} = \frac{(\lambda\|S'\|)^k}{k!} e^{-\lambda\|S'\|}. \tag{11}$$

Moreover, we assume that the orientation of each camera sensor is a random variable with the uniform distribution on $[0, 2\pi]$, i.e., $\theta \sim U(0, 2\pi)$.

Let $L(T)$ be the indicator function indicating whether a point T is *L*-covered or not, i.e.,

$$L(T) = \begin{cases} 1, & \text{if } T \text{ is } L\text{-covered;} \\ 0, & \text{if } T \text{ is not } L\text{-covered,} \end{cases}$$

and let A_L be the *L*-covered area in the deployment region S. Then, we have

$$A_L = \int_S L(T) \mathrm{d}T.$$

We can define the *L*-coverage probability as follows:

Definition 2: L-coverage probability, denoted by P_L. In a deployment field S, the ratio between the mean *L*-covered area and the area of S is said to be the *L*-coverage probability of S, i.e.,

$$P_L \triangleq \frac{\mathrm{E}[A_L]}{\|S\|}, \quad 0 \le P_L \le 1.$$

Remarks on Definition 2: By using the Fubini's theorem [31] and exchange the order of integral and expectation [10], we can get the expected value of A_L as follows:

$$\begin{aligned} \mathrm{E}[A_L] &= \int_S \mathrm{E}[L(T)]\mathrm{d}T = \int_S \Pr\{L(T) = 1\}\mathrm{d}T \\ &= \|S\|\Pr\{L(T) = 1\}, \end{aligned} \tag{12}$$

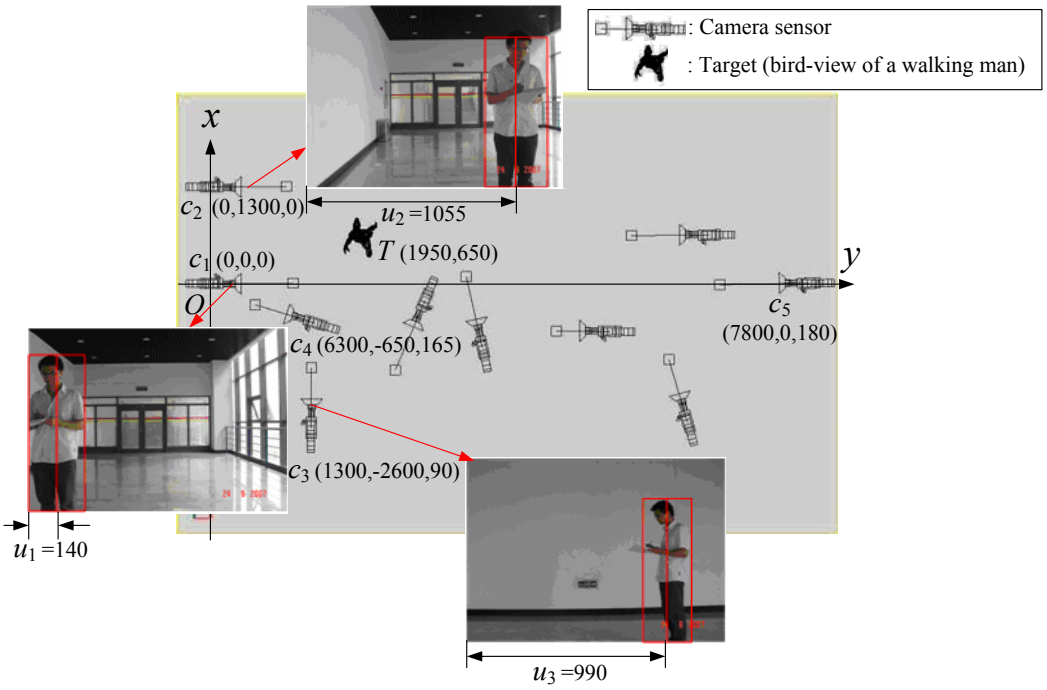

Fig. 4. A scene for illustration of *L*-coverage. There are 10 randomly deployed camera sensors and a target T in a surveillance region. We use three camera sensors, c_1, c_2, and c_3, to capture the images of the target. The $c_i(x_i, y_i, \theta_i), i = 1, 2, 3$ denote the location and orientation of camera sensor c_i, and $u_i, i = 1, 2, 3$ denote the horizontal pixel coordinates of the target.

where $\Pr\{L(T) = 1\}$ is constant for all $T \in S$. According to Eq. (12) and *Definition* 2, the coverage probability is equal to the probability that T is *L*-covered, i.e.,

$$P_L = \Pr\{L(T) = 1\}. \tag{13}$$

The *L*-coverage probability $P_L = 1$ implies that S is completely *L*-covered. However, because the deployment of camera sensors follows the Poisson point process, it is difficult to guarantee $P_L = 1$ for a finite density λ. In this paper, we mainly focus on the relationship between the *L*-coverage probability and the density of camera sensors.

From *Definition 1*, a point $T \in S$ being *L*-covered by k camera sensors implies that 1) there exist k camera sensors which can detect T; and 2) the corresponding δ_k of these k camera sensors is not larger than the predefined threshold ε. Let N_T be the number of camera sensors which can detect T. According to Eq. (13), we have

$$P_L = \sum_{k=1}^{\infty} \Pr\{N_T = k\} \Pr\{\delta_k \le \varepsilon\}, \tag{14}$$

where $\Pr\{N_T = k\}$ is derived by the following lemma.

Lemma 2: If camera sensors are modeled by a two-dimensional stationary Poisson point process with intensity λ, then the probability that there are k camera sensors which can detect T is given by

$$\Pr\{N_T = k\} = \frac{\left(\lambda\alpha r^2\right)^k}{k!} e^{-\lambda\alpha r^2}. \tag{15}$$

Proof: The detailed proof is provided in Appendix II. ■

From *Lemma 2*, we can readily get the expression of *K*-coverage probability for wireless camera sensor networks. In the literature, a point is *K*-covered if it is covered by at least K sensors. Then, in camera sensor networks, the *K*-coverage probability, denoted by P_K, is

$$\begin{aligned} P_K \triangleq \Pr\{N_T \ge K\} &= \sum_{i=K}^{\infty} \frac{\left(\lambda\alpha r^2\right)^i}{i!} e^{-\lambda\alpha r^2} \\ &= 1 - \sum_{i=0}^{K-1} \frac{\left(\lambda\alpha r^2\right)^i}{i!} e^{-\lambda\alpha r^2}. \end{aligned} \tag{16}$$

However, according to Eq. (9), it is difficult to derive the closed-form analytical expression for $\Pr\{\delta_k \le \varepsilon\}$. Next, we study $\Pr\{\delta_k \le \varepsilon\}$ by using Monte Carlo simulations.

Let $T(0, 0)$ be the location of a target. We randomly deploy one camera sensor c in the disk centered around T with the radius r. Let L_c be the location of c, and γ_c be the orientation of $\overrightarrow{L_cT}$. In order to detect T, the orientation θ_c of camera sensor c satisfies the random uniform distribution on $[\gamma_c - \alpha, \gamma_c + \alpha]$. According to Eq. (9), we can get the corresponding δ_1. Assume that ζ, σ_p, and σ_s are fixed, above process is repeated 1000 times to obtain 1000 δ_1's. Define $a \triangleq \varepsilon/r$ and let it vary from 0 to 0.25. For each value of a, we can get the total number, denoted by $N_{L,1}$, of δ_1's which are not larger than corresponding ε. Then, $\Pr\{\delta_1 \le \varepsilon\}$ approximates the ratio of $N_{L,1}$ over 1000.

Figure 5 plots the statistical results of 1000 δ_1's. From Fig. 5, we can observe that about 80% δ_1's are larger than $r/10$. For most applications of wireless camera sensor networks, δ_1 is much larger than ordinary requirements. On the other hand, Eq. (2) shows that it is impossible to derive the unique (x_t, y_t) by using just one measurement. The above observations imply that the point which is covered by *only one camera sensor* cannot generally be *L*-covered. Therefore, we can have the following property:

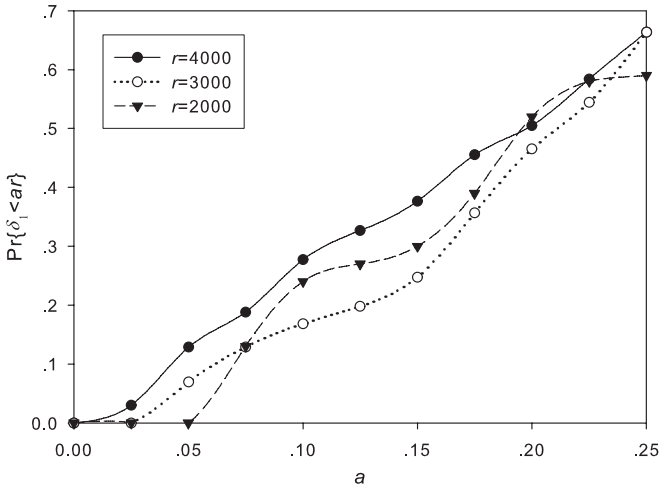

Fig. 5. Relationship between $\Pr\{\delta_1 \leq \varepsilon\}$ and a with different r. We set $\zeta = 5 \times 10^{-8}$, $\sigma_p = 0.1$, and $\sigma_s = 0.1$.

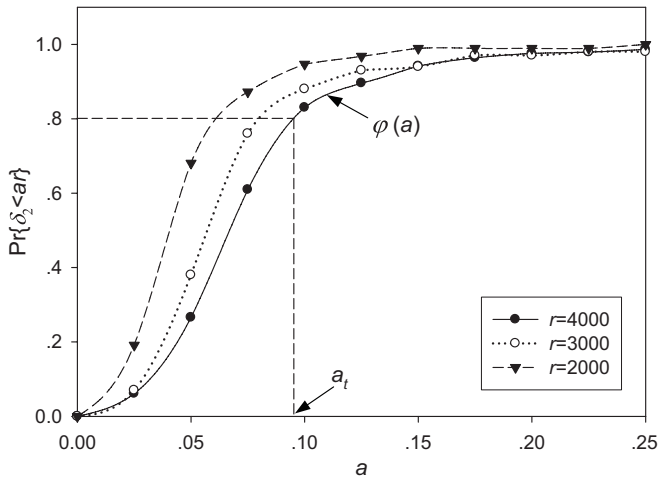

Fig. 6. Relationship between $\Pr\{\delta_2 \leq \varepsilon\}$ and a with different r. We set $\zeta = 5 \times 10^{-8}$, $\sigma_p = 0.1$, and $\sigma_s = 0.1$.

Property 1: The point which is detected by only one camera sensor is not *L*-covered.

Next, we randomly deploy two camera sensors, c_1 and c_2, in the disk centered around T with radius r. Their orientations, θ_1 and θ_2, satisfy the random uniform distribution on $[\gamma_1 - \alpha, \gamma_1 + \alpha]$ and $[\gamma_2 - \alpha, \gamma_2 + \alpha]$, where γ_1 and γ_2 are the orientations of $\overrightarrow{L_1T}$ and $\overrightarrow{L_2T}$, respectively. Then, we can get the corresponding δ_2 according to Eq. (9). We repeat above process 1000 times to obtain 1000 δ_2's. Let a vary from 0 to 0.25 per 0.025 steps. For each value of a, we can get the total number, denoted by $N_{L,2}$, of δ_2's which are not larger than corresponding ε. Then, $\Pr\{\delta_2 \leq \varepsilon\}$ approximate the ratio of $N_{L,2}$ over 1000.

Figure 6 plots the statistical results of 1000 δ_2's. As shown in Fig. 6, when $r = 4000$, about 80% δ_2's are smaller than $r/10$. This implies that if the requirement of localization accuracy is not very strict, then the probability that a point is *L*-covered by two camera sensors, i.e., $\Pr\{\delta_2 \leq \varepsilon\}$, is high. Furthermore, we can also obtain the following observations from Fig. 6:

- When a is at the lower end, $\Pr\{\delta_2 \leq \varepsilon\}$ increases quickly as a increases; when a is at the higher end, $\Pr\{\delta_2 \leq \varepsilon\}$ increases slowly as a increases.
- For a fixed a, $\Pr\{\delta_2 \leq \varepsilon\}$ decreases as r increases.

When $k \geq 3$, it is complicated to calculate δ_k according to Eq. (9), because the dimensions of $\Re$ are large. There is a property for $\Pr\{\delta_k \leq \varepsilon\}$ that $\Pr\{\delta_k \leq \varepsilon\}$ increases as k increases, i.e., $\Pr\{\delta_k \leq \varepsilon\} < \Pr\{\delta_{k+1} \leq \varepsilon\}$. This is because the more camera sensors for estimation, the lower the estimation error. Thus, we have

$$\Pr\{\delta_2 \leq \varepsilon\} < \Pr\{\delta_k \leq \varepsilon\} \leq 1, \text{ for } k > 2.$$

Then, according to Eq. (16), we can obtain

$$\Pr\{\delta_2 \leq \varepsilon\}P_2 < P_L < \Pr\{\delta_2 \leq \varepsilon\}\Pr\{N_T = 2\} + P_3, \quad (17)$$

where

$$P_2 = 1 - e^{-\lambda\alpha r^2} - \lambda\alpha r^2 e^{-\lambda\alpha r^2},$$
$$P_3 = 1 - e^{-\lambda\alpha r^2} - \lambda\alpha r^2 e^{-\lambda\alpha r^2} - \frac{(\lambda\alpha r^2)^2}{2} e^{-\lambda\alpha r^2}.$$

Figure 7 plots $\Pr\{\delta_2 \leq \varepsilon\}P_2$ and $\Pr\{\delta_2 \leq \varepsilon\}\Pr\{N_T = 2\} + P_3$ against λ with two different values of $\Pr\{\delta_2 \leq \varepsilon\}$ by taking $\Pr\{\delta_2 \leq \varepsilon\} = 0.8$ and 0.5, respectively. From Fig. 7, $\Pr\{\delta_2 \leq \varepsilon\}\Pr\{N_T = 2\} + P_3$ approaches to 1 and $\Pr\{\delta_2 \leq \varepsilon\}P_2$ approaches to $\Pr\{\delta_2 \leq \varepsilon\} = 0.8$ or 0.5 when λ goes to infinity. This implies that 1) the difference between $\Pr\{\delta_2 \leq \varepsilon\}P_2$ and $\Pr\{\delta_2 \leq \varepsilon\}\Pr\{N_T = 2\} + P_3$, denoted by ΔP, approaches to $1 - \Pr\{\delta_2 \leq \varepsilon\}$ when λ goes to infinity; 2) ΔP decreases as $\Pr\{\delta_2 \leq \varepsilon\}$ increases. On the other hand, we have

$$\lim_{\lambda\to\infty} \frac{\Pr\{\delta_2 \leq \varepsilon\}P_2}{P_L} = \Pr\{\delta_2 \leq \varepsilon\}$$

and

$$\lim_{\lambda\to\infty} \frac{\Pr\{\delta_2 \leq \varepsilon\}\Pr\{N_T = 2\} + P_3}{P_L} = 1.$$

Therefore, when $\Pr\{\delta_2 \leq \varepsilon\}$ approaches to 1, we can use $\Pr\{\delta_2 \leq \varepsilon\}\Pr\{N_T = 2\} + P_3$ as the approximation of P_L, i.e.,

$$P_L \approx \Pr\{\delta_2 \leq \varepsilon\}\Pr\{N_T = 2\} + P_3.$$

In this paper, we assume that if $\Pr\{\delta_2 \leq \varepsilon\} > 0.8$, then $P_L \approx \Pr\{\delta_2 \leq \varepsilon\}\Pr\{N_T = 2\} + P_3$. However, when ε is at the lower end, $\Pr\{\delta_2 \leq \varepsilon\}$ may be smaller than 0.8. Thus, the difference between P_L and $\Pr\{\delta_2 \leq \varepsilon\}\Pr\{N_T = 2\} + P_3$ cannot be neglected.

Let $\Pr\{\delta_2 \leq \varepsilon\} = \varphi(a)$ be a function of a where $a = \varepsilon/r$. As shown in Fig. 6, we can get the plot of $\varphi(a)$ by using Monte Carlo simulations. Because $\Pr\{\delta_2 \leq \varepsilon\}$ increases monotonically as a increases, we can define a threshold value for a, denoted by a_t, as follows: $a_t \triangleq \inf\{a \mid \varphi(a) \geq 0.8\}$. If $\varepsilon < a_t r$, i.e., $a < a_t$, then $\Pr\{\delta_2 \leq \varepsilon\} < 0.8$. Define

$$r' \triangleq \frac{\varepsilon}{a_t}. \quad (18)$$

Substituting $r = r'$ into Eq. (9), Eq. (15), and Eq. (16), we can get the corresponding δ_2, $\Pr\{N_T = 2\}$, and P_K with the sensing radius r', denoted by δ_2', $\Pr\{N_T' = 2\}$, and P_K', respectively. Let $\varphi'(a)$ be the function which expresses the

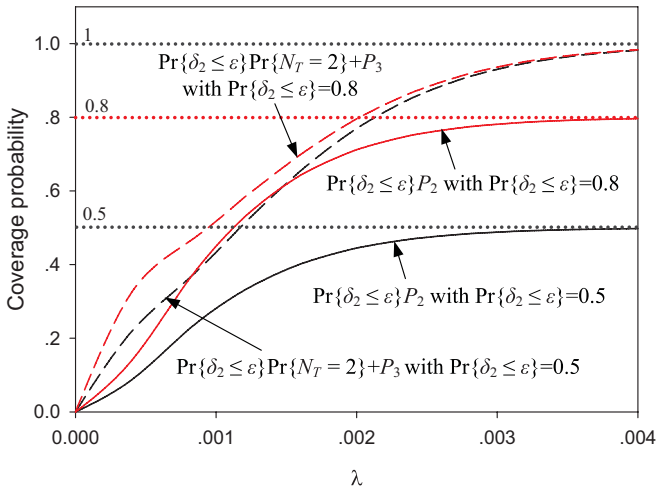

Fig. 7. The curves of $\Pr\{\delta_2 \le \varepsilon\}P_2$ and $\Pr\{\delta_2 \le \varepsilon\}\Pr\{N_T = 2\} + P_3$ when $\Pr\{\delta_2 \le \varepsilon\} = 0.8$ and 0.5, respectively.

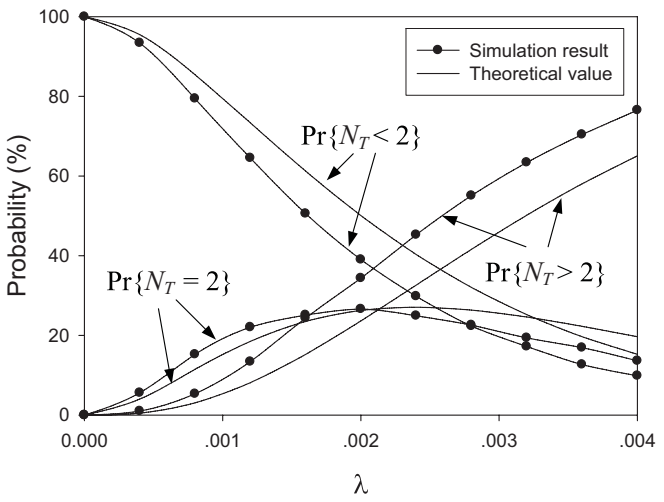

Fig. 8. Comparisons between the simulation results and the analytical results of $\Pr\{N_T < 2\}$, $\Pr\{N_T = 2\}$, and $\Pr\{N_T > 2\}$, where $r = 40$.

relationship between $\Pr\{\delta_2' \le \varepsilon\}$ and a. Because $\Pr\{\delta_2 \le \varepsilon\}$ decreases as r increases, $\varphi'(a_t) > 0.8$. This implies that

$$P_L \approx \Pr\{\delta_2' \le \varepsilon\}\Pr\{N_T' = 2\} + P_3'.$$

We can also use Monte Carlo simulations to get the curve of $\varphi'(a)$. However, in order to simplify the computation, we use $P_2' \approx \Pr\{N_T' = 2\}\Pr\{\delta_2' \le \varepsilon\} + P_3'$, because $\Pr\{\delta_2' \le \varepsilon\} > 0.8$. Therefore, we can derive the approximated expression for P_L as follows:

$$P_L \approx \begin{cases} 1 - e^{-\lambda\alpha r^2} - \lambda\alpha r^2 e^{-\lambda\alpha r^2} \\ \quad - \left(1 - \varphi\left(\frac{\varepsilon}{r}\right)\right)\frac{(\lambda\alpha r^2)^2}{2} e^{-\lambda\alpha r^2}, & \text{if } \varepsilon > a_t r; \\ 1 - e^{-\lambda\alpha\left(\frac{\varepsilon}{a_t}\right)^2} \\ \quad -\lambda\alpha\left(\frac{\varepsilon}{a_t}\right)^2 e^{-\lambda\alpha\left(\frac{\varepsilon}{a_t}\right)^2}, & \text{otherwise.} \end{cases} \tag{19}$$

From Eq. (19), we can obtain the corresponding density of camera sensors for a given L-coverage probability.

VI. Simulation Experiments

We verify our derived model and analytical analyses on the L-coverage in wireless camera sensor networks through simulation experiments. In order to perform empirical evaluations of the L-coverage probability, we have built up a simulation platform by using VC++. The fixed parameters of the simulation platform are as follows: $S = 500 \times 500$, $\alpha = \pi/6$, $\zeta = 5 \times 10^{-8}$, $\sigma_p = 0.1$, and $\sigma_s = 0.1$.

In each simulation run, we randomly scatter a number of camera sensors according to a 2-dimensional Poisson process with mean $\lambda \times 250000$ within S. The number of camera sensors, N, varies from 0 to 1000 per 100 steps. A grid of 500×500 vertices is created for S. From *Property 1*, when a point is covered by only one camera sensor, this point cannot be L-covered. This implies that the region which is covered by only one camera sensor is also the vacancy for L-coverage. Then, we can divide these 250,000 vertices into three categories: 1) the vertices covered by 0 or 1 camera sensor, 2) the vertices covered by 2 camera sensors, and 3) the vertices covered by at least 3 camera sensors. Assume that there are n vertices which are covered by 0 or 1 camera sensor. We repeat above process 100 times to obtain the mean of n, $\mathrm{E}[n]$, for each value of λ. Then, the simulation result of $\Pr\{N_T < 2\}$ is computed as the ratio between $\mathrm{E}[n]$ and 250,000. By using the same method, we can also get the simulation results of $\Pr\{N_T = 2\}$ and $\Pr\{N_T > 2\}$.

Figure 8 plots the simulation results and analytical results of $\Pr\{N_T < 2\}$, $\Pr\{N_T = 2\}$, and $\Pr\{N_T > 2\}$ against λ. As shown in Fig. 8, the analytical results of $\Pr\{N_T < 2\}$ are always slightly larger than simulation results. The analytical results of $\Pr\{N_T > 2\}$ are slightly smaller than simulation results. $\Pr\{N_T = 2\}$ increases at first, and then decreases as λ increases. The analytical results of $\Pr\{N_T = 2\}$ are slightly larger than simulation results during the increasing process of $\Pr\{N_T = 2\}$, and are slightly smaller than simulation results during the decreasing process. These observations imply that:

- For $\Pr\{N_T < 2\}$, $\Pr\{N_T = 2\}$, and $\Pr\{N_T > 2\}$, the simulation results are close to the analytical results;
- In order to obtain a given coverage probability, the simulation results for λ are slightly smaller than the analytical results.

For each value of λ, we randomly generate 20 different topologies of camera sensors. In each topology, we compute the corresponding δ_2 for all the vertices covered by 2 camera sensors. The threshold ε takes the value of 0,1,...,10. Assume that there exist n' vertices which satisfy $\delta_2 \le \varepsilon$. Then, we can get the ratio between n' and the number of vertices which are covered by 2 cameras. Repeat this process 20 times to obtain the mean of this ratio, i.e., the simulation result of $\Pr\{\delta_2 \le \varepsilon\}$. Table III summarizes the simulation results and analytical results of $\Pr\{\delta_2 \le \varepsilon\}$. We can also observe that the simulation results are very close to the corresponding analytical results.

Set $\varepsilon = 4$, we can get the simulation results of P_L by substituting the simulation results of $\Pr\{N_T = 2\}$, $\Pr\{N_T > 2\}$, and $\Pr\{\delta_2 \le \varepsilon\}$ into Eq. (13). As shown in Fig. 9, the simulation results of P_L are slightly larger than analytical results. As λ increases, the difference between the simulation result and the corresponding analytical result increases firstly, and then decreases. On the other hand, for each value of λ, we

TABLE III
COMPARISON BETWEEN SIMULATION RESULTS (THE NUMBERS IN THE COLUMNS 2 THROUGH 11) AND ANALYTICAL RESULTS (THE NUMBERS IN THE COLUMN 12) OF $\Pr\{\delta_2 \leq \varepsilon\}$.

	λ (for simulation results)										
ε	0.0004	0.0008	0.0012	0.0016	0.0020	0.0024	0.0028	0.0032	0.0036	0.0040	Analytical results
100	.0500	.0522	.0426	.0571	.0652	.0500	.0424	.0447	.0468	.0349	.0611
200	.3400	.2410	.1782	.2368	.2301	.2421	.2263	.2481	.1959	.1968	.2659
300	.6600	.5663	.5798	.5666	.5471	.6184	.5758	.6328	.5205	.5873	.6092
400	.8900	.8032	.8032	.7949	.8225	.8395	.8121	.8685	.8041	.8222	.8302
500	.9400	.8795	.8936	.8858	.8986	.9132	.9051	.9330	.9035	.8984	.8958
600	.9500	.9116	.9335	.9302	.9420	.9395	.9414	.9578	.9240	.9365	.9416
700	.9800	.9357	.9574	.9577	.9583	.9632	.9677	.9752	.9561	.9460	.9641
800	.9800	.9558	.9734	.9725	.9692	.9816	.9758	.9851	.9649	.9587	.9757
900	.9900	.9719	.9814	.9831	.9873	.9895	.9818	.9950	.9766	.9714	.9793
1000	1.0000	.9839	.9920	.9873	.9946	.9974	.9859	.9975	.9825	.9873	.9865

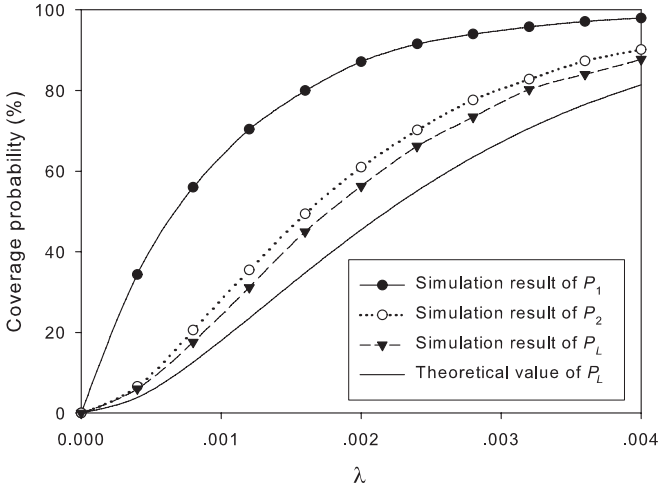

Fig. 9. Comparisons among 1-coverage probability (P_1), 2-coverage probability (P_2), and L-coverage probability (P_L).

compare the simulation results of P_1 and P_2 to the simulation result of P_L, respectively. From Fig. 9, we can observe that P_L is much smaller than P_1 (P_1, i.e., 1-coverage probability, is the ordinary coverage probability for detecting applications). Because $\Pr\{\delta_2 \leq 4\}$ is about 80%, P_L is slightly smaller than P_2.

We can obtain the simulation results of $\Pr\{\delta_2 \leq \varepsilon\}P_2$ and $\Pr\{N_T = 2\}\Pr\{\delta_2 \leq \varepsilon\} + P_3$ by using the simulation results of $\Pr\{\delta_2 \leq \varepsilon\}$, $\Pr\{N_T = 2\}$, P_2, and P_3. Even the difference, ΔP, between $\Pr\{\delta_2 \leq \varepsilon\}P_2$ and $\Pr\{N_T = 2\}\Pr\{\delta_2 \leq \varepsilon\} + P_3$ increases as λ increases, ΔP is always small when ε is at the higher end (Fig. 10(a)). Therefore, P_L approximates to $\Pr\{N_T = 2\}\Pr\{\delta_2 \leq \varepsilon\} + P_3$. Figure 10(a) also shows that ΔP decreases as ε increases. If ε is small, i.e., the application has a strict restriction on localization accuracy, then $\Pr\{\delta_2 \leq \varepsilon\}$ is small, and the ΔP is large (Fig. 10(b)). According to Eq. (18), we use $r' = 20$ as the sensing radius of camera sensors, and then get the corresponding P_2'. As shown in Fig. 10(b), the difference between P_2' and $\Pr\{\delta_2 \leq \varepsilon\}P_2$ is small, i.e., P_L can approximate to P_2'. We notice that the simulated $\Pr\{\delta_2 \leq \varepsilon\}P_2$ is not always less than P_2', which is because of the limited number of simulations.

VII. CONCLUSIONS

We investigated the coverage problem from the perspective of target localization in wireless camera sensor networks, which is necessary to make camera sensor networks useful for surveillance applications. We proposed and analyzed the novel localization-oriented sensing model based on the perspective projection model of camera. We formulated the problem of localization in the framework of Bayesian estimation, and proposed a new notion of localization-oriented coverage (L-coverage). Furthermore, we analyzed the relationships between L-coverage probability and the density of camera sensors, and derived the requirement density of camera sensors for an expected L-coverage probability. Our proposed system models and schemes were validated and evaluated through the extensive simulation experiments.

APPENDIX A
PROOF OF *Lemma* 1

The MSE of $\widehat{T}_k$ is

$$\begin{aligned}\mathrm{MSE}(\widehat{T}_k) &= \mathrm{E}[(x_t - \widehat{x})^2 + (y_t - \widehat{y})^2] \\ &= \int\int_S \left[(\widehat{x} - x_t)^2 + (\widehat{y} - y_t)^2\right] f(t|\mathbf{X})\mathrm{d}x\mathrm{d}y.\end{aligned}$$

To minimize the $\mathrm{MSE}(\widehat{T}_k)$, we take its partial derivative over $\widehat{x}$ and $\widehat{y}$, respectively, as follows:

$$\begin{aligned}&\tfrac{\partial}{\partial \widehat{x}}\left(\int\int_S \left[(\widehat{x} - x_t)^2 + (\widehat{y} - y_t)^2\right] f(t|\mathbf{X})\mathrm{d}x\mathrm{d}y\right) \\ &\quad = \int\int_S \tfrac{\partial}{\partial \widehat{x}}\left(\left[(\widehat{x} - x_t)^2 + (\widehat{y} - y_t)^2\right] f(t|\mathbf{X})\right)\mathrm{d}x\mathrm{d}y \\ &\quad = -2\int\int_S (x_t - \widehat{x}) f(t|\mathbf{X})\mathrm{d}x\mathrm{d}y. \\ &\tfrac{\partial}{\partial \widehat{y}}\left(\int\int_S \left[(\widehat{x} - x_t)^2 + (\widehat{y} - y_t)^2\right] f(t|\mathbf{X})\mathrm{d}x\mathrm{d}y\right) \\ &\quad = \int\int_S \tfrac{\partial}{\partial \widehat{y}}\left(\left[(\widehat{x} - x_t)^2 + (\widehat{y} - y_t)^2\right] f(t|\mathbf{X})\right)\mathrm{d}x\mathrm{d}y \\ &\quad = -2\int\int_S (y_t - \widehat{y}) f(t|\mathbf{X})\mathrm{d}x\mathrm{d}y.\end{aligned}$$

Setting the above partial derivatives to be zeros and solving them, respectively, we get

$$\begin{cases} \widehat{x} = \int\int_S x f(t|\mathbf{X})\mathrm{d}x\mathrm{d}y, \\ \widehat{y} = \int\int_S y f(t|\mathbf{X})\mathrm{d}x\mathrm{d}y. \end{cases} \tag{20}$$

Then, substituting Eq. (7) into Eq. (20), we obtain Eq. (8).

APPENDIX B
PROOF OF *Lemma* 2

From the sensing model of camera sensors, it is easy to know that if a camera sensor can detect T, then the location of this camera sensor must be in the disk, denoted by R, which is centered around T with radius r. On the other hand, not all

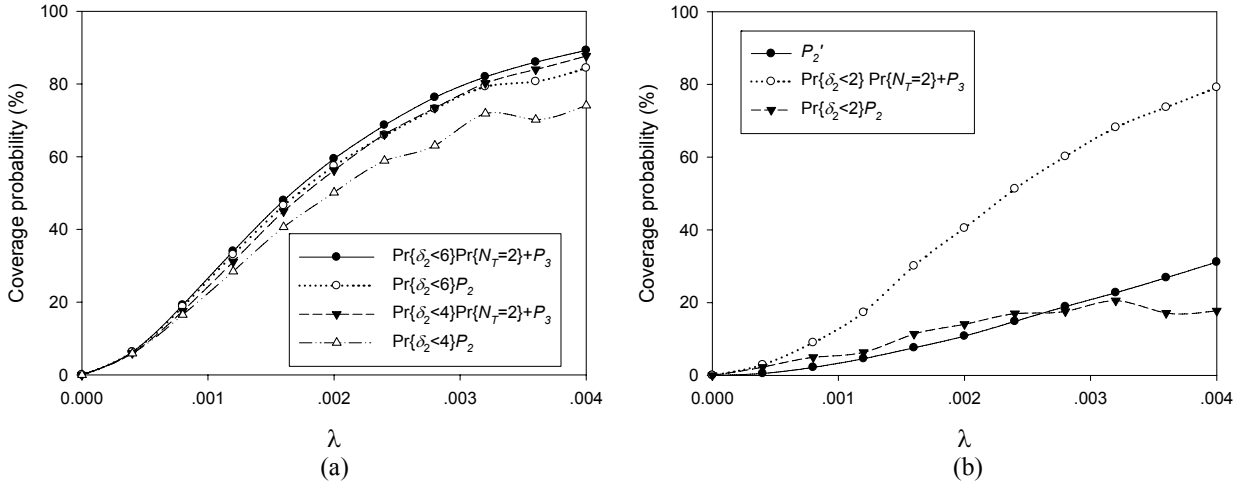

Fig. 10. (a) The differences among $\Pr\{\delta_2 \leq 6\}P_2$, $\Pr\{N_T = 2\}\Pr\{\delta_2 \leq 6\} + P_3$, $\Pr\{\delta_2 \leq 4\}P_2$, and $\Pr\{N_T = 2\}\Pr\{\delta_2 \leq 4\} + P_3$; (b) the differences among $\Pr\{\delta_2 \leq 2\}P_2$, $\Pr\{N_T = 2\}\Pr\{\delta_2 \leq 2\} + P_3$, and P_2'. We set $r = 40$ and $r' = 20$.

camera sensors in R can detect T because of their orientations. Assume that there are n camera sensors in R, from Eq. (11), we have

$$\Pr\{N_R = n\} = \frac{(\lambda\pi r^2)^n}{n!} e^{-\lambda\pi r^2},$$

where N_R is the number of the cameras sensors in R. The probability that a camera sensor in R can detect T is α/π. Then, the probability that k $(k \leq n)$ of these n camera sensors can detect the target T is

$$\Pr\{N_T = k | N_R = n\} = \left(\frac{\alpha}{\pi}\right)^k \left(1 - \frac{\alpha}{\pi}\right)^{n-k} \left(\begin{array}{c} n \\ k \end{array} \right).$$

Then,

$$\begin{aligned} &\Pr\{N_T = k\} \\ &= \sum_{n=k}^{\infty} \Pr\{N_R = n\}\Pr\{N_T = k | N_R = n\} \\ &= \sum_{n=k}^{\infty} \frac{(\lambda\pi r^2)^n}{n!} e^{-\lambda\pi r^2} \left(\frac{\alpha}{\pi}\right)^k \left(1 - \frac{\alpha}{\pi}\right)^{n-k} \left(\begin{array}{c} n \\ k \end{array} \right) \\ &= \frac{\left(\lambda\alpha r^2\right)^k}{k!} e^{-\lambda\alpha r^2}, \end{aligned}$$

which is Eq. (15).

REFERENCES

[1] I. F. Akyildiz, T. Melodia, and K. Chowdhury, "Wireless multimedia sensor networks: a survey," *Computer Networks*, vol. 51, pp. 921-960, 2007.

[2] P. Kulkarni, D. Ganesan, P. Shenoy, and Q. Lu, "SensEye: a multi-tier camera sensor network," in *Proc. 13th Annual ACM International Conference on Multimedia*, Nov. 2005, pp. 229-238.

[3] H. Ma and D. Tao, "Multimedia sensor network and its research progresses," *J. Software*, vol. 17, pp. 2013-2028, 2006.

[4] R. Holman, J. Stanley, and T. Ozkan-Haller, "Applying video sensor networks to nearshore environment monitoring," *IEEE Perv. Comput.*, vol. 2, pp. 14-21, 2003.

[5] J. Campbell, P. B. Gibbons, S. Nath, P. Pillai, S. Seshan, and R. Sukthankar, "IrisNet: an Internet-scale architecture for multimedia sensors," in *Proc. 13th Annual ACM International Conference on Multimedia*, Nov. 2005, pp. 81-88.

[6] S. Denman, C. Fookes, J. Cook, C. Davoren, A. Mamic, G. Farquharson, D. Chen, B. Chen, and S. Sridharan, "Multi-view intelligent vehicle surveillance system," in *Proc. IEEE International Conference on Video and Signal Based Surveillance (AVSS '06)*, Nov. 2006, pp. 26-26.

[7] M. Bramberger, A. Doblander, A. Maier, B. Rinner, and H. Schwabach, "Distributed embedded smart cameras for surveillance applications," *Computer*, vol. 39, pp. 68-75, Feb. 2006.

[8] M. Li, Y. Liu, and L. Chen, "Non-threshold based event detection for 3D environment monitoring in sensor networks," *IEEE Trans. Knowledge and Data Engineer.*, vol. 20, pp. 1699-1711, Dec. 2008.

[9] B. Wang, W. Wang, V. Srinivasan, and K. C. Chua, "Information coverage for wireless sensor networks," *IEEE Commun. Lett.*, vol. 9, pp. 967-969, Nov. 2005.

[10] B. Wang, K. C. Chua, V. Srinivasan, and W. Wang, "Information coverage in randomly deployed wireless sensor networks," *IEEE Trans. Wireless Commun.*, vol. 6, no. 8, pp. 2994-3004, Aug. 2007.

[11] B. Wang, K. C. Chua, V. Srinivasan, and W. Wang, "Sensor density for complete information coverage in wireless sensor networks," in *Proc. EWSN2006*, Feb. 2006, pp. 69-82.

[12] P. Hall, *Introduction to the Theory of Coverage Processes*. John Wiley & Sons, 1988.

[13] S. Meguerdichian, F. Koushanfar, M. Potkonjak, and M.Srivastava, "Coverage problems in wireless ad-hoc sensor network," in *Proc. 20th IEEE INFOCOM*, Mar. 2001, pp. 1380-1387.

[14] S. Shakkottai, R. Srikant, and N. B. Shroff, "Unreliable sensor grids: coverage, connectivity and diameter," in *Proc. IEEE INFOCOM2003*, Apr. 2003, pp. 1073-1083.

[15] P. Wan and C. Yi, "Coverage by randomly deployed wireless sensor networks," *IEEE Trans. Inf. Theory*, vol. 52, no. 6, pp. 2658-2669, June 2006.

[16] M. Liu, J. Cao, Y. Zheng, L. Chen, and L. Xie, "Analysis for multi-coverage problem in wireless sensor networks," *J. Software*, vol. 18, pp. 127-136, 2007.

[17] X. Wang, G. Xing, Y. Zhang, C. Lu, R. Pless, and C. Gill, "Integrated coverage and connectivity configuration in wireless sensor networks," in *Proc. ACM Sensys*, Nov. 2003, pp. 28-39.

[18] C. Huang and Y. Tseng, "The coverage problem in a wireless sensor network," in *Proc. WSNA*, Sep. 2003, pp. 115-121.

[19] H. Zhang and J. Hou, "On deriving the upper bound of α-lifetime for large sensor networks," in *Proc. ACM International Symposium on Mobile Ad Hoc Networking and Computing (MobiHoc)*, May 2004, pp. 121-132.

[20] H. Ma and Y. Liu, "Some problems of directional sensor networks," *International J. Sensor Networks*, vol. 2, no. 1-2, pp. 44-52, Apr. 2007.

[21] D. Tao, H. Ma, and L. Liu, "Coverage-enhancing algorithm for directional sensor networks," in *Proc. 2nd Int'l Conf. on Mobile Ad-Hoc and Sensor Networks (MSN'06)*, Dec. 2006, pp. 256-267.

[22] D. Tao, H. Ma, and L. Liu, "A virtual potential field based coverage-enhancing algorithm for directional sensor networks," *J. Software*, vol. 18, pp. 1152-1163, 2007.

[23] E. Hörster and R. Lienhart, "Approximating optimal visual sensor placement," in *Proc. IEEE ICME2006*, July 2006, pp. 1257-1260.
[24] E. Hörster and R. Lienhart, "On the optimal placement of multiple visual sensors," in *Proc. 4th ACM International Workshop on Video Surveillance and Sensor Networks (VSSN2006)*, Oct. 2006, pp. 111-120.
[25] S. Rama, K. R. Ramakrishnan, P. K. Atrey, V. K. Singh, and M. S. Kankanhalli, "A design methodology for selection and placement of sensors in multimedia surveillance system," in *Proc. 4th ACM International Workshop on Video Surveillance and Sensor Networks (VSSN2006)*, Oct. 2006, pp. 121-130.
[26] J. Elson, L. Girod, and D. Estrin, "Fine-grained network time synchronization using reference broadcasts," in *Proc. 5th Symp. on Operating Systems Design and Implementation*, 2002, pp. 147-163.
[27] A. O. Ercan, D. B.-R. Yang, A. El Gamal, and L. J. Guibas, "Optimal placement and selection of camera network nodes for target localization," in *Proc. DCOSS2006*, June 2006, pp. 389-404.
[28] M. Piccardi, "Background subtraction techniques: a review," in *Proc. IEEE International Conference on Systems, Man and Cybernetics*, Oct. 2004, pp. 3099-3104.
[29] K. Kim, T. H. Chalidabhongse, D. Harwood, and L. S. Davis, "Real-time foreground-background segmentation using codebook model," *Real-Time Imaging*, vol. 11, pp. 172-185, June 2005.
[30] Q. Wang, W. Chen, R. Zheng, K. Lee, and L. Sha, "Acoustic target tracking using tiny wireless sensor devices," in *Proc. ACM IPSN2003*, Apr. 2003, pp. 642-657.
[31] G. B. Thomas and R. L. Finney, *Calculus and Analytic Geometry*, 8th edition. Addison-Wesley, 1996.

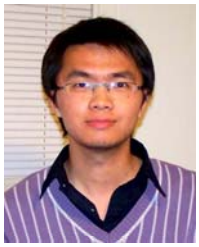

Liang Liu is an assistant professor of Beijing Key Lab of Intelligent Telecommunications Software and Multimedia, Beijing University of Posts and Telecommunications, China. He received the Ph.D. degree from Department of Computer, Beijing University of Posts and Telecommunications, China, in 2009 and the B.S. degree from the Department of Computer Science and Technology, South China University of Technology, China, in 2004. He was a visiting Ph.D. student in the Networking and Information Systems Laboratory, Texas A&M University, USA during 2007-2008. His research interests are in the fields of wireless sensor networks, camera sensor networks, and information theory.

Xi Zhang (S'89-SM'98) received the B.S. and M.S. degrees from Xidian University, Xi'an, China, the M.S. degree from Lehigh University, Bethlehem, PA, all in electrical engineering and computer science, and the Ph.D. degree in electrical engineering and computer science (Electrical Engineering-Systems) from The University of Michigan, Ann Arbor.

He is currently an Associate Professor and the Founding Director of the Networking and Information Systems Laboratory, Department of Electrical and Computer Engineering, Texas A&M University, College Station. He was an Assistant Professor and the Founding Director of the Division of Computer Systems Engineering, Department of Electrical Engineering and Computer Science, Beijing Information Technology Engineering Institute, China, from 1984 to 1989. He was a Research Fellow with the School of Electrical Engineering, University of Technology, Sydney, Australia, and the Department of Electrical and Computer Engineering, James Cook University, Australia, under a Fellowship from the Chinese National Commission of Education. He worked as a Summer Intern with the Networks and Distributed Systems Research Department, AT&T Bell Laboratories, Murray Hills, NJ, and with AT&T Laboratories Research, Florham Park, NJ, in 1997. He has published more than 140 research papers in the areas of wireless networks and communications systems, mobile computing, network protocol design and modeling, statistical communications, random signal processing, information theory, and control theory and systems.

Prof. Zhang received the U.S. National Science Foundation CAREER Award in 2004 for his research in the areas of mobile wireless and multicast networking and systems. He received the Best Paper Award in the IEEE Globecom 2007. He also received the TEES Select Young Faculty Award for Excellence in Research Performance from the Dwight Look College of Engineering at Texas A&M University, College Station, in 2006. He is currently serving as an Editor for the IEEE TRANSACTIONS ON WIRELESS COMMUNICATIONS, an Associate Editor for the IEEE TRANSACTIONS ON VEHICULAR TECHNOLOGY, a Guest Editor for the IEEE JOURNAL ON SELECTED AREAS IN COMMUNICATIONS for the special issue on "wireless video transmissions," an Associate Editor for the IEEE COMMUNICATIONS LETTERS, an Editor for the John Wiley's *Journal on Wireless Communications and Mobile Computing*, an Editor for the *Journal of Computer Systems, Networking, and Communications*, and an Associate Editor for the John Wiley's *Journal on Security and Communications Networks*, and is also serving as the Guest Editor for the *IEEE Wireless Communications Magazine* for the special issue on "next generation of CDMA versus OFDMA for 4G wireless applications" and a Guest Editor for John Wiley's *Journal on Wireless Communications and Mobile Computing* for the special issue on "next generation wireless communications and mobile computing." He has frequently served as the Panelist on the U.S. National Science Foundation Research-Proposal Review Panels. He is serving or has served as the TPC Chair for IEEE Globecom 2011, TPC Vice-Chair for IEEE INFOCOM 2010, Co-Chair for IEEE INFOCOM 2009 - Mini-Conference, Co-Chair for IEEE Globecom 2008 - Wireless Communications Symposium, Co-Chair for the IEEE ICC 2008 - Information and Network Security Symposium, Symposium Chair for IEEE/ACM International Cross-Layer Optimized Wireless Networks Symposium 2006, 2007, and 2008, respectively, the TPC Chair for IEEE/ACM IWCMC 2006, 2007, and 2008, respectively, the Poster Chair for IEEE INFOCOM 2008, the Student Travel Grants Co-Chair for IEEE INFOCOM 2007, the Panel Co-Chair for IEEE ICCCN 2007, the Poster Chair for IEEE/ACM MSWiM 2007 and IEEE QShine 2006, Executive Committee Co-Chair for QShine, the Publicity Chair for IEEE/ACM QShine 2007 and IEEE WirelessCom 2005, and the Panelist on the Cross-Layer Optimized Wireless Networks and Multimedia Communications at IEEE ICCCN 2007 and WiFi-Hotspots/WLAN and QoS Panel at IEEE QShine 2004. He has served as the TPC members for more than 70 IEEE/ACM conferences, including IEEE INFOCOM, IEEE Globecom, IEEE ICC, IEEE WCNC, IEEE VTC, IEEE/ACM QShine, IEEE WoWMoM, IEEE ICCCN, etc. Prof. Zhang is a Senior Member of the IEEE and a Member of the Association for Computing Machinery (ACM).

Huadong Ma is a Professor and Director of Beijing Key Lab of Intelligent Telecommunications Software and Multimedia, Chair of Department of Computer Science and Technology, Beijing University of Posts and Telecommunications, China. He received his Ph.D. degree in Computer Science from Institute of Computing Technology, Chinese Academy of Science in 1995, M.S. degree in Computer Science from Shenyang Institute of Computing Technology, Chinese Academy of Science in 1990 and B.S. degree in Mathematics from Henan Normal University in 1984. He visited UNU/IIST as research fellow in 1998 and 1999, respectively. From 1999 to 2000, he held a visiting position in the Department of Electrical Engineering and Computer Science, The University of Michigan, Ann Arbor, Michigan. He was a visiting Professor at The University of Texas at Arlington from July to September 2004, and a visiting Professor at Hong Kong University of Science and Technology from Dec. 2006 to Feb. 2007. His current research focuses on multimedia system and networking, sensor networks and grid computing, and he has published over 100 papers and four books on these fields. He is member of IEEE and ACM.